Journal of ELECTRONIC MATERIALS, Vol. 41, No. 6, 2012
DOI: 10.1007/s11664-012-2036-3

Improvement of Electrical Contact Between TE Material and Ni Electrode Interfaces by Application of a Buffer Layer

KOYA ARAI,[1,3] MASANORI MATSUBARA,[1] YUKIE SAWADA,[1]
TATSUYA SAKAMOTO,[1] TOHRU KINERI,[2] YASUO KOGO,[1]
TSUTOMU IIDA,[1] and KEISHI NISHIO[1,4]

1.—Department of Materials Science and Technology, Tokyo University of Science, 2641 Yamazaki, Noda-shi, Chiba 278-8510, Japan. 2.—Department of Applied Chemistry, Tokyo University of Science, Yamaguchi, 1-1-1 Daigaku-Dori, Sanyoonoda-shi, Yamaguchi 756-0884, Japan. 3.—e-mail: j8210604@ed.tus.ac.jp. 4.—e-mail: k-nishio@rs.noda.tus.ac.jp

A single π-structure thermoelectric (TE) module based on p-type $NaCo_2O_4$, n-type Mg_2Si, and Ni electrode was fabricated by the spark plasma sintering (SPS) method. The $NaCo_2O_4$ powder was synthesized by using a metal–citric acid complex decomposition method. Bulk Mg_2Si prepared by melt quenching was ground into a powder and sieved to particle size of 75 μm or less. To obtain a sintered body of $NaCo_2O_4$ or Mg_2Si, the powder was sintered using SPS. Pressed Ni powder or mixed powder consisting of Ni and $SrRuO_3$ powder was inserted between these materials and the Ni electrode in order to connect them, and electrical power was passed through the electrodes from the SPS equipment. The open-circuit voltage (V_{OC}) values of a single module in which TE materials were connected to the Ni electrodes by using pressed Ni powder was 82.7 mV, and the maximum output current (I_{max}) and maximum output power (P_{max}) were 212.4 mA and 6.65 mW at $\Delta T = 470$ K, respectively. On the other hand, V_{OC} of a single module in which TE materials and an Ni electrode were connected with a mixed powder (Ni:$SrRuO_3$ = 6:4 volume fraction) was 109 mV, and I_{max} and P_{max} were 4034 mA and 109 mW at $\Delta T = 500$ K, respectively. These results indicate that the resistance at the interface between the TE materials and the Ni electrode can be decreased and the output power can be increased by application of a buffer layer consisting of Ni and $SrRuO_3$.

Key words: $NaCo_2O_4$, Mg_2Si, $SrRuO_3$, thermoelectric module, spark plasma sintering

INTRODUCTION

Thermoelectric (TE) power generation has recently attracted much interest as a technology for conversion of heat into electricity. High-performance TE modules based on intermetallic compounds have been studied intensively in recent years.[1,2] Additionally, some modules based on Bi-Te intermetallic compounds have already been put to practical use.[3,4] On the other hand, TE modules based on metal oxides have also been studied widely. However, there are few reports of such modules that have high performance when compared with TE modules based on intermetallic compounds. In this paper, we describe the fabrication of π-structure TE modules based on $NaCo_2O_4$ and Mg_2Si.

Metal oxides are thermally more stable and less harmful than intermetallic compounds such as Bi_2Te_3. Furthermore, metal oxide is better in terms of ease of preparation and control of chemical composition. Many researchers are looking for TE materials that can provide high thermopower, low resistivity, and low thermal conductivity. Recently, layered cobalt oxides, i.e., Na-Co-O and Ca-Co-O,

---

(Received July 16, 2011; accepted March 1, 2012;

have been shown to have low resistivity and low thermal conductivity.[5–12] $NaCo_2O_4$ and $Ca_3Co_4O_9$ consist of Na ions or Ca_2CoO_3 and CoO_2 blocks stacked alternately along the *c*-axis to form a layered structure.[13] Thus, the physical properties are highly two-dimensional in the *a*–*b* plane compared with the *c*-axis direction. These materials are promising for TE applications at high temperatures in air. In particular, Co-based oxides that have a layered structure (i.e., $NaCo_2O_4$ and $CaCo_4O_9$) are good *p*-type thermoelectric oxide materials.[5,6] The preparation of fine $NaCo_2O_4$ powder by the metal–citric acid complex decomposition method,[14] and highly oriented $NaCoO_4$ ceramics prepared by the SPS method have been reported.[15] On the other hand, magnesium silicide (Mg_2Si) has been identified as a promising TE material for use at operating temperatures from 500 K to 800 K. The dimensionless figure of merit, ZT, which is used to characterize the efficiency of TE materials, has already reached $\sim$1.0 at 873 K for *n*-type Mg_2Si.[16] A large number of studies have investigated the TE characteristics of Mg_2Si, and the output characteristics of Mg_2Si and associated modules have been reported by Iida and others.[17–19] Therefore, we fabricated a π-structure TE module with $NaCo_2O_4$ as the *p*-type leg and Mg_2Si as the *n*-type leg by using the spark plasma sintering (SPS) method.[15] However, the module had high contact resistance, which usually occurs at the interface between $NaCo_2O_4$ and Ni electrodes. Contact resistance at the interface between the semiconductor and the metal electrode is a serious problem in many TE modules.[20,21] In particular, oxide–metal junctions cause high contact resistance. Accordingly, some reports on the fabrication of oxide-based TE modules show that their performance is much lower than expected;[22,23] for example, electrodes made of silver pastes containing different contents of oxide powders have been reported to improve the electrical contacts.[24,25] In this study, we tried to improve the modules by the introduction of a buffer layer consisting of Ni and $SrRuO_3$, and the TE performance of the modules was evaluated. $SrRuO_3$ has high thermal stability and high resistance to chemical corrosion, and its perovskite-type crystal structure favors integration with other oxides that have high potential in technological applications, such as superconductors or ferroelectrics.[26,27] It is expected that interface resistance will be decreased by applying the buffer layer.

EXPERIMENTAL PROCEDURES

$NaCo_2O_4$ powder was prepared using a modified Pechini's method.[28] Pechini's method is a simple way of preparing metal oxide powders.[29,30] This process offers several advantages for the fabrication of metal oxide powders, including low cost, homogeneous composition, high purity, and low heat-treatment temperatures. The precursor solutions were prepared from metal salts [CH_3COONa and $Co(NO_3)_2{\cdot}6H_2O$], citric acid, and ethylene glycol monomethyl ether. These metal salts were dissolved in a solution of the citric acid and the ethylene glycol monomethyl ether. The solution was refluxed at 333 K for 1 h. After drying at 378 K, the precursor solution was heated at 723 K for 2 h. To obtain the plate-like precursor powder, the dried powder was heat-treated at 1173 K in air for 1 h.

$SrRuO_3$ powder was also prepared using the modified Pechini's method. The precursor solutions were prepared from metal salts [$Sr(CH_3COO)_2{\cdot}0.5H_2O$ and $RuCl_3{\cdot}H_2O$], citric acid, and H_2O. These metal salts were dissolved with a solution of citric acid and H_2O in N_2 atmosphere. The precursor solution was heated at 823 K for 5 h after being dried at 353 K for 8 h to obtain the precursor powder. To obtain $SrRuO_3$ as a single-phase powder, the dried powder was heat-treated at 1273 K in air for 5 h.

Presynthesized polycrystalline Mg_2Si was provided by Union Material Inc. The presynthesized Mg_2Si was prepared from a mixture of high-purity Mg (99.95 %) and Si (99.99999 %) at stoichiometric ratio of Mg:Si = 2:1, and it was heat-treated in an electrical furnace. The bulk polycrystalline Mg_2Si was ground to a powder and sieved to particle size of 75 μm or less.

Spark plasma sintering (SPS) was carried out using a DR. SINTER LAB 515S system (SPS Syntex, Inc., Japan). For the SPS, the precursor powder was placed in a graphite die and heat-treated up to a predefined temperature ($NaCo_2O_4$: 1073 K, Mg_2Si: 1123 K) at a rate of 100 K/min, after which it was maintained at that temperature for 5 min under uniaxial pressure of 60 MPa in Ar atmosphere (1013 hPa). After attaining and holding the sintering temperature in the SPS process, the electrical power was turned off at the holding temperature, and the sample was cooled to room temperature in the SPS chamber. The sintered blocks were cut and polished. The relative densities of the samples were measured using the Archimedes method.

The thermoelectric elements for the *I*–*V* measurements of the $NaCo_2O_4$ ceramics with Ni electrodes or composite electrodes consisted of Ni and $SrRuO_3$ (Ni:$SrRuO_3$ = 6:4 by volume fraction). Figure 1 shows an illustration and a photo of a thermoelectric element. The *I*–*V* measurements were carried out using the standard four-probe method (ULVAC-RIKO, ZEM-2) in He atmosphere.

The specific contact resistance was measured by the four-probe method. Figure 2 shows an illustration of the specific contact resistance measurement by four-probe method and a photo of the sample. The sample was fabricated using SPS equipment. The samples consisted of $NaCo_2O_4$ (5.0 mm × 10.0 mm × 6.0 mm), Ni powder or mixed powder (Ni:$SrRuO_3$ = 6:4 by volume fraction), and Ni plate electrode (5.0 mm × 10.0 mm × 0.5 mm). To connect the $NaCo_2O_4$ and the electrode, either pressed Ni powder or mixed

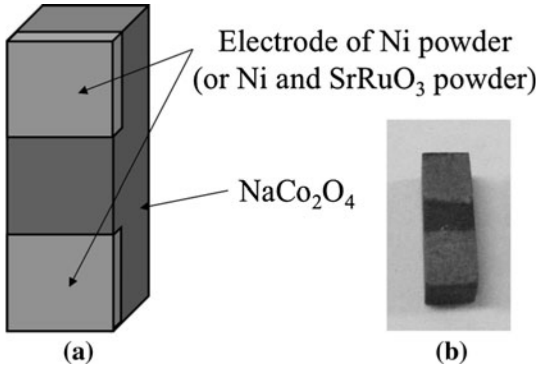

Fig. 1. (a) Illustration and (b) photo of the thermoelectric element.

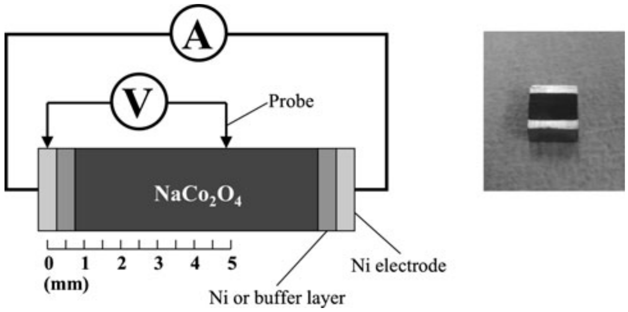

Fig. 2. Illustration of specific contact resistance measurement by four-probe method and a photo of the sample.

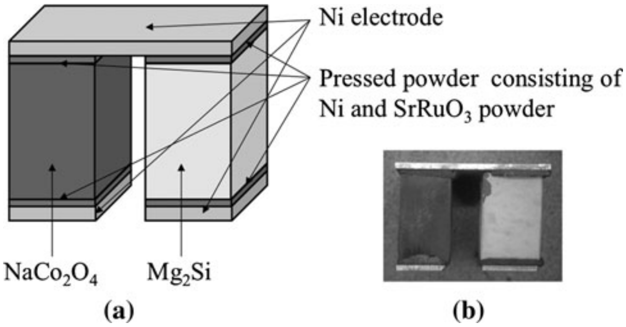

Fig. 3. (a) Illustration and (b) photo of the TE module.

powder was put between the Ni plate electrodes and the NaCo$_2$O$_4$ sintered body, and then electrical power was applied between the Ni plate/pressed Ni or the powder mixture/sintered body/pressed Ni or the powder mixture/Ni plate in the SPS chamber.

The thermoelectric module was fabricated using SPS equipment. The TE module consisted of NaCo$_2$O$_4$ (4.95 mm × 11.9 mm × 7.7 mm) as the *p*-type semiconductor, Mg$_2$Si (5.5 mm × 11.95 mm × 7.7 mm) as the *n*-type semiconductor, Ni plates (13.0 mm × 13.0 mm × 0.5 mm) as the electrodes for the hot top, and Ni plates (5.5 mm × 13.0 mm × 0.5 mm) as the electrodes for the cold bottom (Fig. 3). To connect the TE elements and the electrodes, either pressed Ni powder or mixed powder (Ni:SrRuO$_3$ = 6:4 by volume fraction) was put between the Ni plate electrodes and the NaCo$_2$O$_4$ or Mg$_2$Si sintered body, and then electrical power was applied between the Ni plate/pressed Ni or the powder mixture/sintered body/pressed Ni or the powder mixture/Ni plate in the SPS chamber.

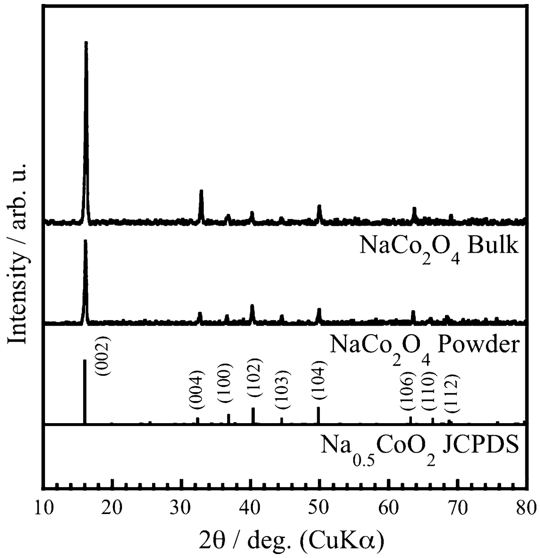

Fig. 4. XRD patterns of NaCo$_2$O$_4$ powder, ceramics, and a JCPDS reference.

The open-circuit voltage and the thermoelectric power outputs of π-structure modules with temperature differences, ΔT, ranging from 100 K to 500 K were measured in air using a Union Material UMTE-1000 M. The top of the module was heated by an electrically heated stainless-steel block, whereas the base was cooled using an aluminum block. The heat that was applied to the heating block came from an electrical heater working at 473 K to 873 K, whereas the cooling block was maintained at 373 K by a combination of water cooling and electrical heating. The output current and output power were measured under closed-circuit conditions by varying the value of the external load.

RESULTS AND DISCUSSION

Figure 4 shows the XRD patterns of the NaCo$_2$O$_4$ powder, the ceramics, and a JCPDS reference. Comparing the diffraction patterns of the powder and the ceramics with those of the reference, one can see that the peaks of the (00*l*) phases were more intense than those of the other phases. The XRD measurements indicated that the *c*-axis of the prepared NaCo$_2$O$_4$ ceramic was perpendicular to the uniaxial pressure direction. The degree of texture was evaluated in terms of the Lotgering factor,[11]

$$f = (p - p_0)/(1 - p_0), \quad (1)$$

where

$$p = \Sigma I_{(00l)}/\Sigma I_{(hkl)} \tag{2}$$

for the diffraction pattern of the sample, and $p = p_0$ for a randomly oriented powder diffraction pattern of the reference. The Lotgering factor of the sample was above 50 %. Scanning electron microscopy (SEM) revealed that the $NaCo_2O_4$ particles had a plate-like shape and a high aspect ratio. The theoretical relative densities of the $NaCo_2O_4$ and the Mg_2Si sintered body were above 98 %.

Figure 5 shows current–voltage curves for $NaCo_2O_4$ with Ni electrodes (a), and for $NaCo_2O_4$ with "mixture" electrodes (Ni:$SrRuO_3$ = 6:4) (b). The voltages of the samples were measured by changing the current over the temperature range from 373 K to 973 K in increments of 50 K. In the low-temperature range (up to 623 K), the electrical properties of $NaCo_2O_4$ with Ni electrodes could not be measured because a high-resistance barrier (i.e., a Schottky barrier junction) was formed at the interface between the sample and the Ni electrodes, whereas the resistivity of the sample could be measured above 673 K (Fig. 5a). The resistivity of the sample decreased nonlinearly with increasing measurement temperature. According to the results, it seems that the current for the $NaCo_2O_4$-Mg_2Si TE module decreased significantly on the cold side. On the other hand (Fig. 5b), investigations of the *I*–*V* curves could be carried out above 373 K when a buffer layer was inserted at the interface between the $NaCo_2O_4$ and the Ni electrodes. It is believed that much lower electrical resistance contacts than between the $NaCo_2O_4$ and the Ni can be formed between $SrRuO_3$ and Ni, and $SrRuO_3$ and $NaCo_2O_4$, respectively, and that the interface resistivity decreases as a result. The temperature dependence of the electrical resistivity (ρ) was calculated from the current–voltage curves shown in Fig. 5a, b. The theoretical electric resistivity (ρ) of the thermoelectric elements can be expressed as

$$\rho = R_{\mathrm{cal}} S/l, \tag{3}$$

where R_{cal} is calculated from the value of the slope of the line of the current–voltage curve (contributing rate >0.97). S and l are the cross-section of the thermoelectric element and the distance between the electrodes, respectively. As shown in Fig. 6, the electrical resistivity of the thermoelectric element with a buffer layer included decreased significantly relative to the element without the buffer layer. The value of the electrical resistivity decreased to about 1/30th at 873 K. It seems that the electrical conductive path provided by $SrRuO_3$ made it possible for the thermoelectric element to have high electrical conductivity at low temperature.

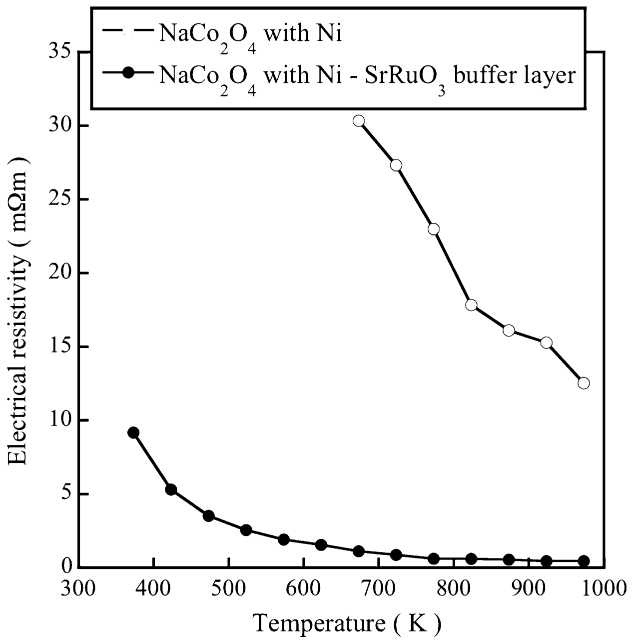

Fig. 6. Temperature dependence of electrical resistivity.

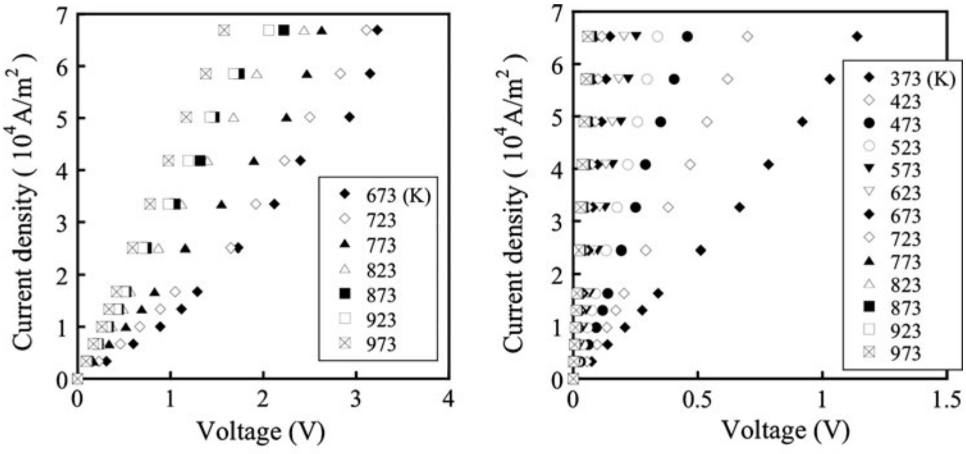

(a) (b)

Fig. 5. Current–voltage curves of an $NaCo_2O_4$-Ni thermoelectric element: (a) without and (b) with a buffer layer.

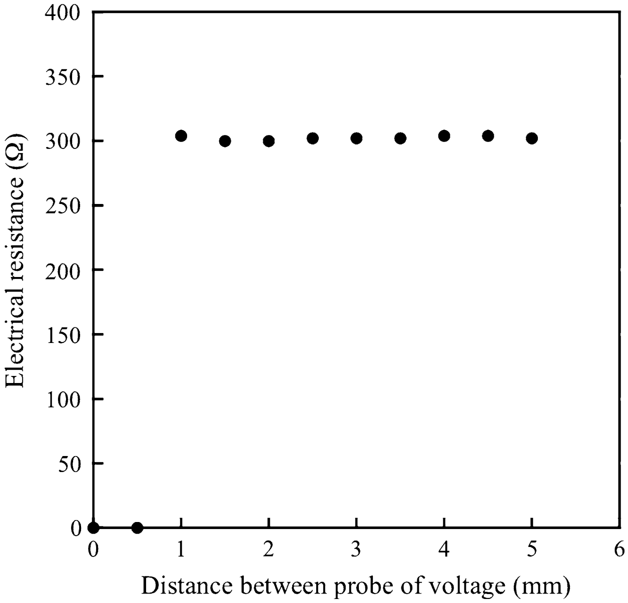

Fig. 7. Specific contact resistance measurements between Ni and $NaCo_2O_4$.

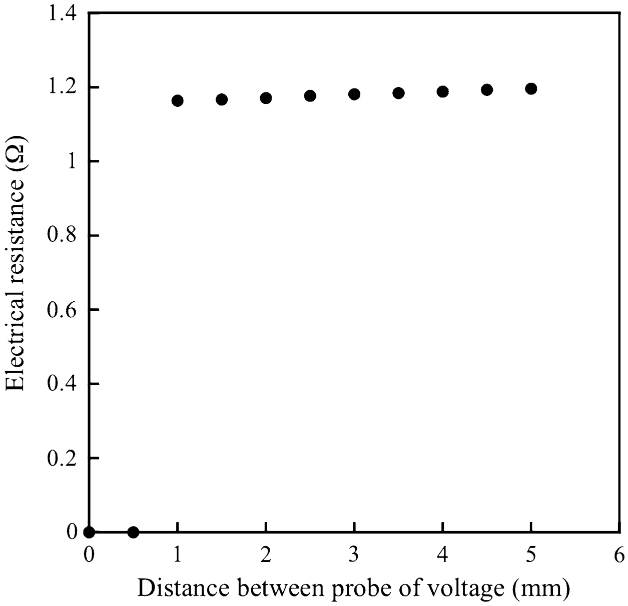

Fig. 8. Specific contact resistance measurements between Ni and buffer layer ($Ni{:}SrRuO_3 = 6{:}4$ by volume fraction), and between buffer layer and $NaCo_2O_4$.

Figure 7 shows specific contact resistance measurements between Ni and $NaCo_2O_4$. Figure 8 shows specific contact resistance measurements between the Ni and buffer layer ($Ni{:}SrRuO_3 = 6{:}4$ by volume fraction), and between the buffer layer and $NaCo_2O_4$. It seems that there is no (negligibly low) contact resistance between the Ni and buffer layer. The value of the specific contact resistivity between the electrode and $NaCo_2O_4$ decreased to about 1/260th at room temperature by inserting the buffer layer.

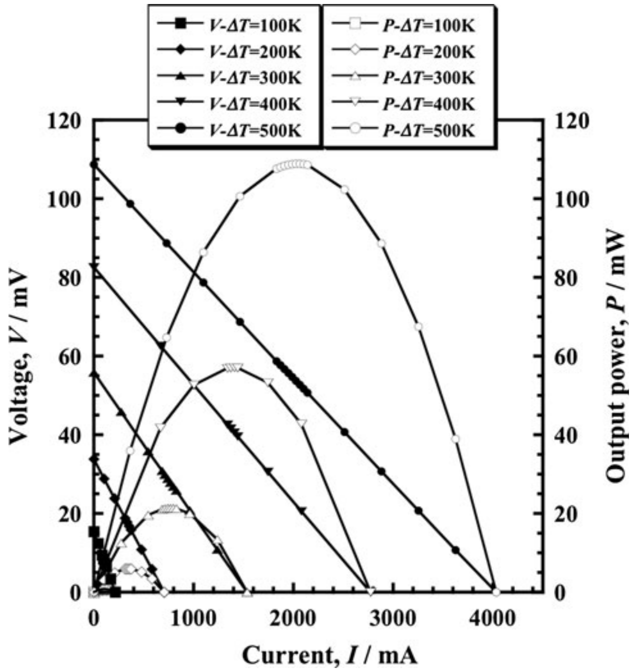

Fig. 9. I–V characteristics and output power of the module versus temperature differences, ΔT, ranging from 100 K to 500 K.

Figure 9 shows the I–V and I–P curves for the $NaCo_2O_4$-Mg_2Si TE module with the buffer layer for various temperature differences, ΔT, ranging from 100 K to 500 K. Under the same temperature conditions, the external resistance (R_{ex}) of the circuit changed from R_{ex} = maximum (open circuit) to 0 [voltage (V) = 0]. The open-circuit voltage (V_{OC}) is measured at R_{ex} = maximum. The maximum output current (I_{max}) is measured at $R_{ex} = 0$. On the other hand, the output power increased with decreasing external resistance, and exhibited a maximum value of output power (P_{max}) at $V = V_{OC}/2$ [current (I) = $I_{max}/2$], and then decreased and reached zero at $V = 0$ ($I = I_{max}$). The maximum value of V_{OC} reached 109 mV at $\Delta T = 500$ K. The obtained maxima, I_{max} and P_{max}, for the single module were 4034 mA and 109 mW, respectively, at $\Delta T = 500$ K. Table I presents the thermoelectric performance of two single TE modules. One of these is a module without a buffer layer that we fabricated previously,[15] and the other was fabricated as part of this work. The output power at high temperature ($\Delta T = 500$ K, 470 K) of the latest module was more than 16 times higher than the module that we fabricated in the past. This is believed to be due to a decrease in contact resistance at the interface between the $NaCo_2O_4$ thermoelectric material and the Ni electrode due to the insertion of the buffer layer. Moreover, the buffer layer produced a marked improvement in the electrical conductivity at low temperature (ΔT =100 K). It seems that the electrical conductive path of $SrRuO_3$ enables high electrical conductivity at low temperature.

Table I. Thermoelectric performance of the single π-structure TE modules

	Element Dimensions (mm)	ΔT (K)	V_{OC} (mV)	I_{max} (mA)	P_{max} (mW)	$P_{max}/\Delta T$ (mW/K)
This work	p: 4.95 × 11.9 × 7.7 n: 5.5 × 11.95 × 7.7	500	109	4034	109	0.218
No buffer layer[15]	p: 4.75 × 9.4 × 8.55 n: 5.4 × 10.5 × 8.55	470	82.7	212.4	6.65	0.0141

Table II. Thermoelectric performance results for reported oxide modules

Author	Materials	Element Dimensions (mm)	p–n Couples	ΔT (K)	V_{OC} (V)	P_{max} (mW)	$P_{max}/\Delta T$ (mW/K)
This work	p: $NaCo_2O_4$ n: Mg_2Si	4.95 × 11.9 × 7.7 5.5 × 11.95 × 7.7	1	500	0.109	109	0.218
Souma et al.[31]	p: $NaCo_2O_4$ n: ZnO		12	455	0.79	52.5	0.115
Funahashi and Urata[21]	p: $Ca_{2.7}Bi_{0.3}Co_4O_9$ n: $La_{0.9}Bi_{0.1}NiO_3$	1.3 × 1.3 × 5	140	551	4.5	150	0.272
Funahashi and Urata[21]	p: $Ca_{2.7}Bi_{0.3}Co_4O_9$ n: $La_{0.9}Bi_{0.1}NiO_3$	3.7 × 4–4.5 × 4.7	8	565	1	170	0.301
Choi et al.[32]	p: $Ca_3Co_4O_9$ n: $(ZnO)_7In_2O_3$	15 × 15 × 27 15 × 15 × 18	44	673	1.8	423	0.629

Table II presents the reported thermoelectric performance results for oxide-based modules. The thermoelectric performance results of the modules with p-type $NaCo_2O_4$ and n-type Mg_2Si couples were reported by us. The open-circuit voltage (0.109 V) of this work is the lowest value among those reported to date. For this reason, the module reported in this work has only one p–n junction. However, the maximum value of output power (109 mW) in this work is by far the highest value for a single module (one p–n junction). Therefore, it can be expected that improvements could be realized by connecting the modules described in this work in order to generate increased electrical power.

CONCLUSIONS

A thermoelectric module with a π structure consisting of p-type $NaCo_2O_4$ and n-type Mg_2Si has been successfully fabricated by SPS. With the insertion of a mixed powder (Ni:$SrRuO_3$ = 6:4 by volume fraction) buffer layer, the electrical resistivity of the $NaCo_2O_4$–Ni element was reduced to about 1/30th of previous levels at 873 K. The open-circuit voltage of a single module with an $SrRuO_3$–Ni buffer layer was 109 mV, and the maximum output current and maximum output power were 4034 mA and 109 mW at ΔT = 500 K, respectively.

REFERENCES

1. B. Poudel, Q. Hao, Y. Ma, Y. Lan, A. Minnich, B. Yu, X. Yan, D. Wang, A. Muto, D. Vashaee, X. Chen, J. Liu, M.S. Dreselhaus, G. Chen, and Z. Ren, *Science* 320, 634 (2008). doi:10.1126/science.1156446.
2. D. Kraemer, B. Poudel, H. Feng, J.C. Caylor, B. Yu, X. Yan, Y. Ma, X. Wang, D. Wang, A. Muto, K. McEnaney, M. Chiesa, Z. Ren, and G. Chen, *Nat. Mater.* 10, 532 (2011). doi: 10.1038/NMAT3013.
3. T. Kajikawa, *J. Electron. Mater.* 38, 1083 (2009).
4. H. Hachiuma and K. Fukuda, *Proceedings of the 5th European Conference on Thermoelectrics* (2007). Available: http//ect2007.thermion-company.com/proc.contents.
5. I. Terasaki, Y. Sasago, and K. Uchinokura, *Phys. Rev.* B56, R12685 (1997).
6. H. Yakabe, K. Kikuchi. I. Terasaki, Y. Sasago, and K. Uchinokura, *Proceedings of the 16th International Conference on Thermoelectrics* (1997), p. 523.
7. T. Itoh, T. Kawata, T. Kitajima, and I. Terasaki, *Proceedings of the 17th International Conference on Thermoelectrics* (1998), p. 567.
8. I. Terasaki, *Proceedings of the 19th International Conference on Thermoelectrics* (2000), p. 20.
9. S. Li, R. Funahashi, I. Matsubara, K. Ueno, S. Sodeoka, and H. Yamada, *J. Mater. Chem.* 9, 1659 (1999).
10. S. Li, R. Funahashi, I. Matsubara, K. Ueno, S. Sodeoka, and H. Yamada, *Chem. Mater.* 12, 2424 (2000).
11. S. Tajima, T. Tani, S. Isobe, and K. Koumoto, *Mater. Sci. Eng. B* 86, 20 (2001).
12. Y.W. Gu, K.A. Khor, and P. Cheang, *Biomaterials* 25, 4127 (2004).
13. D. Wang, L. Chen, Q. Yao, and J. Li, *Solid State Commun.* 129, 615 (2004).
14. M. Ito, Y. Oda, and S. Hara, *J. Jpn. Soc. Powder Metall.* 50, 952 (2003).
15. K. Arai, H. Akimoto, T. kineri, T. Iida, and K. Nishio, *Key Eng. Mater., Vol. 485, Electroceramics in Japan XIV* (2011), pp. 169-172.
16. M. Fukano, T. Iida, K. Makino, M. Akasaka, Y. Oguni, and Y. Takanashi, *Mater. Res. Soc. Symp. Proc.*, Vol. 1044, ed. T.P. Hogan, J. Yang, R. Funahashi, and T.M. Tritt (2008), p. 247.
17. Y. Oguni, T. Iida, A. Matsumoto, T. Nemoto, J. Onosaka1, H. Takaniwa, T. Sakamoto, D. Mori1, M. Akasaka, J. Sato, T. Nakajima, K. Nishio, and Y. Takanashi, *Mater. Res. Soc.*

Symp. Proc., Vol. 1044, ed. T.P. Hogan, J. Yang, R. Funahashi, and T.M. Tritt (2008), p. 413.

18. T. Nemoto, T. Iida, Y. Oguni, J. Sato, A. Matsumoto, T. Sakamoto, T. Miyata, T. Nakajima, H. Taguchi, K. Nishio, and Y. Takanashi, *Mater. Res. Soc. Symp. Proc.*, Vol. 1166, ed. J. Yang, G.S. Nolas, K. Koumoto, and Y. Grin (2009), p. 141.
19. T. Nemoto, T. Iida, J. Sato, Y. Oguni, A. Matsumoto, Y. Miyata, T. Sakamoto, T. Nakajima, H. Taguchi, K. Nishio, and Y. Takanashi, *J. Electron. Mater.* 39, 1572 (2010).
20. H. Su, Y. Jiang, X. Lan, X. Liu, H. Zhong, and D. Yu, *Phys. Status Solidi A* 208, 147 (2011).
21. R. Funahashi and S. Urata, *Int. J. Appl. Ceram. Technol.* 4, 297 (2007).
22. I. Matsubara, R. Funahashi, T. Takeuchi, S. Sodeoka, T. Shimizu, and K. Ueno, *Appl. Phys. Lett.* 78, 3627 (2001).
23. W. Shin, N. Murayama, K. Ikeda, and S. Sago, *J. Power Sources* 103, 80 (2001).
24. R. Funahashi, S. Urata, K. Mizuno, T. Kouuchi, and M. Mikami, *Appl. Phys. Lett.* 85, 1036 (2004).
25. R. Funahashi, M. Mikami, T. Mihara, S. Urata, and N. Ando, *J. Appl. Phys.* 99, 066117-1 (2006).
26. J. Roldan, F. Sanchez, V. Trik, C. Guerrero, F. Benitez, C. Ferrater, and M. Varela, *Appl. Surf. Sci.* 154/155, 159 (2000).
27. T. Kodaira, K. Nishio, I. Yamaguchi, S. Suzuki, K. Tsukada, and T. Tsuchiya, *J. Sol–Gel. Sci. Technol.* 26, 1049 (2003).
28. M.P. Pechini, U.S. patent 333,0697 (1967).
29. K. Nishio, T. Okada, N. Kikuchi, S. Mikusu, T. Iida, K. Tokiwa, T. Watanabe, and T. Kineri, *Mater. Res. Soc. Symp. Proc.*, Vol. 116 (2009), p. 1166-N03-13.
30. H. Takenouchi, T. Imai, H. Mae, M. Fujimoto, T. Kineri, T. Iida, N. Hamada, T. Watanabe, and K. Nishio, *Materials Research Society Symposium Proceedings* (2008) p. 1044-U06-11.
31. T. Souma, M. Ohtaki, K. Ohnishi, M. Shigeno, Y. Ohba, and T. Shimozaki, *Proceeding of the 26th International Conference on Thermoelectrics* (2007), p. 38.
32. S. Choi, K. Lee, C. Lim, and W. Seo, *Energy Convers. Manage.* 52, 335 (2011).